Electroreduction of nitrate and carbon dioxide on copper electrodes: a mechanistic study

Perez Gallent, E.

Chapter 3

Structure-sensitive electroreduction of acetaldehyde to ethanol on copper and its mechanistic implications for CO and CO_2 reduction

Ethanol is a highly desirable product of the electrochemical reduction of CO and/or CO2 on copper. Although ethanol and ethylene share common intermediates at the early stages of CO/CO2 reduction to C2 species on copper, the pathways bifurcate and most copper surfaces favor the formation of ethylene. We present here a combined experimental-computational study of the electroreduction of acetaldehyde to ethanol on Cu(111), Cu(100) and Cu(322). The experiments show structure-sensitive onset potentials for acetaldehyde reduction such that lower overpotentials are observed for more open facets (η322 < η 100 < η 111). Our DFT calculations show that the electrochemical reduction of acetaldehyde proceeds via a CH3CH2O* intermediate on the three electrodes at high *H coverage, and that the stability of this weakly bound intermediate determines the onset potential. Our results suggest that during the late stages of CO/CO2 reduction to C2 species on copper, ethanol formation has higher energetic barriers than ethylene formation, and hence the selectivity is inclined towards the latter. Importantly, our results suggest that the barriers for ethanol formation can be lowered by making use of its structure sensitivity.

This chapter has been published as: I Ledezma-Yanez, E Pérez-Gallent, MTM Koper, F Calle-Vallejo, Catalysis Today, 2016, 262, 90-94

3.1 Introduction

It is well known that CO and CO_2 can be reduced electrochemically to useful products. The seminal works of Hori and co-workers pointed out that copper is a unique catalyst for electrochemical CO_2 reduction [105-106], as it is able to produce methane, ethylene and ethanol in different proportions depending on the electrode potential and morphology. However, substantial overpotentials and low Faradaic efficiencies prevent the widespread use of electrolyzers based on copper electrocatalysts. Currently, the challenges are, first of all, to achieve a thorough understanding of the intricate multielectron reaction mechanism, and secondly, to design efficient and selective catalysts based on such understanding.

The major C_2 product on copper is ethylene, while there is a marginal production of ethanol and traces of acetaldehyde [105-106]. There are several indications that these three products share the same reaction pathway up to a given key intermediate, the ease of protonation of which ultimately determines the selectivity [107-108]. Given that in the context of a solar-fuel-based economy ethanol is a highly desirable product, it is important to understand the mechanistic features of its formation, as the C_2 selectivity is usually inclined towards ethylene instead of ethanol. However, Kanan and co-workers have shown recently that the selectivity of copper-based electrocatalysts for CO reduction can be steered to favor ethanol over ethylene [48], although the atomic-scale justification for such a change is still unclear.

According to previous work from our group [107-109], acetaldehyde reduction corresponds to the late stages of the reaction pathway of ethanol production from CO/CO_2. Thus, the study of acetaldehyde reduction reaction can shed light on the features of copper electrodes that may favor ethanol production, as well as provide design principles to devise new catalysts that are selective towards ethanol.

In this chapter, we present a combined experimental/theoretical study of acetaldehyde reduction, taking into account pH effects and structure sensitivity. Our findings provide new insights on the reaction mechanism through which ethanol is produced on copper-based catalysts and help explain why ethylene is the major C_2 product of the reduction of CO/CO_2.

3.2 Experimental

Prior to the experiments, all the glassware was cleaned by boiling in a sulfonitric solution, which is a mixture of concentrated sulfuric acid and nitric acid in a 3:1 ratio. After the acid bath, the glassware was rinsed and boiled five times with ultra-clean water (Milipore® MiliQ; resistivity >18.2 MΩ).

The electrochemical measurements were carried out using an METROHM μAUTOLABIII - Compact Design potentiostat connected to the three-electrode cell. The working electrodes (WE) were bead-type copper single crystals, with a polishing orientation < 0.5 degrees. These electrodes were electropolished before each experiment, using 66% H_3PO_4 (Suprapur Merck) at 2.3 V vs a Cu counter electrode for 2 s, and in open circuit potential (OCP) for 30 s. After cleaning and rinsing with water, the electrode surfaces were characterized by performing four cycles between -0.25 and 0.35 V_{RHE}, at 50 mV s^{-1} in 0.1 M NaOH (Sigma–Aldrich TraceSelect), following the procedure described previously by Schouten et al on Cu single-crystal characterization [110], see Appendix II, Figure AII.1. The results show that the electrodes possessed their distinctive features before the electroreduction experiments. However, we do not discard H- or OH-induced surface reconstruction under reaction conditions.

The counter electrode (CE) consisted of a gold wire, while the reference electrode (RE) was a reversible hydrogen electrode (RHE). All potentials in this work are reported against the RHE, unless otherwise stated.

The experiments were carried out in a solution containing 0.1 M $HClO_4$ (Suprapur Merck) for pH1, and 0.001 M $HClO_4$ + 0.099 M $KClO_4$ (Sigma-Aldrich TraceSelect) for pH 3. These values of pH are used to guarantee the stability of acetaldehyde, which is prone to decomposition in alkaline conditions. All solutions were prepared with ultra-clean water. Argon (Linde, 6.0) was used as purge gas.

The detection of ethanol from the reduction of 0.1 M acetaldehyde (puriss. p.a., anhydrous, ≥99.5% (GC) FLUKA) was monitored by means of online High Performance Liquid Chromatography (HPLC) [111] in a three-electrode cell containing solutions with pH 1 and 3, prepared as previously described. The soluble reduction products were detected by collecting from the solution in the cell using a Teflon tip (0.38 mm in diameter) by means of a fraction collector (FRC-10A, Shimadzu) during the voltammetric scan at a scan rate of 1 mV s^{-1}. The tip was positioned in parallel configuration, approximately 10 μm from the middle of the electrode surface. The fractions collected were deposited in a 96-well microtiter plate. The flow rate of sample collection was adjusted to 60 μL min^{-1} with a Shimadzu pump (LC-20AT). Each of the samples collected were 60 μL. The well was placed in the autosampler, and 30 μL of sample was injected in the high-performance liquid chromatography (HPLC) column. The column used was an Aminex HPX 87-H, Biorad. The temperature of the column was maintained at 85 °C in an oven (CTO-20 A).

3.3 Computational details

The DFT calculations and thermodynamic modeling in this study have been performed using the same methodologies used in our previous work [107]. Here we provide a brief description of the methods used: all adsorption energies were calculated by means of DFT calculations using the VASP code [112] with the PBE exchange-correlation functional [113] and the projector augmented wave (PAW) method [114]. The (111), (100) and

(322) surfaces of copper were modeled with 4-layer-thick slabs. Cu(111) and Cu(100) used 3×2 supercells, while Cu(322) is 5(111)×(100) with a 3-atom wide step edge. The vertical separation between periodically repeated images was more than 16 Å and, additionally, dipole corrections were applied. The structures were optimized allowing the adsorbates and the two topmost layers to relax in all directions, while fixing the 2 bottom layers at the optimized bulk positions, where the lattice constant is 3.64 Å. The relaxations were carried out with a plane-wave cut-off of 400 eV, using the conjugate-gradient scheme until the maximum force on any atom was below 0.05 eV $Å^{-1}$. The Brillouin zones of the (100) and (111) surfaces were sampled with 6×8×1 Monkhorst-Pack meshes [115], while a 4×3×1 mesh was used for the (322) surface. The Fermi level of the surfaces was smeared using the Methfessel-Paxton method [116] with an electronic temperature of 0.2 eV, and all energies were extrapolated to T = 0 K. Acetaldehyde (CH_3CHO) and ethanol (CH_3CH_2OH) were calculated in boxes of 15 Å ×15 Å × 15 Å, with an electronic temperature of 0.001 eV, the gamma point only, and Gaussian smearing. The free energies are estimated from DFT-calculated energies in the following way:

$$G = E_{DFT} + ZPE - TS \quad (3.1)$$

The zero-point energies (ZPE) of the adsorbates (see Table 3.1) and molecules (1.468 and 2.118 eV for CH_3CHO and CH_3CH_2OH) were calculated from vibrational frequency analysis using the harmonic oscillator approximation. Vibrational contributions to the entropy were considered only for adsorbed species and can be found in Table 3.1, while total entropies for molecules were taken from standard thermodynamic tables at 298.15 K and 1 bar [117], so that the gas-phase *TS* corrections for ethanol and acetaldehyde are 0.870 and 0.815 eV, respectively. However, ethanol and acetaldehyde are liquid at the conditions of the experiments carried out here. Although it is normally difficult to estimate the liquid-phase free energies of substances within standard DFT, there is a simple thermodynamic workaround [107, 118-119]. Essentially, the substance is simulated in the gas phase and the

difference between the free energies of formation of its liquid and gas phases is added to the gas-phase entropy. Such differences are 0.072 eV for ethanol and -0.056 eV for acetaldehyde, so that the final TS corrections are 0.942 and 0.759 eV, respectively. The high-coverage (HC) situations on the (111), (100) and (322) surfaces contained 5, 5, and 4 *H coadsorbates around CH_3CH_2O*/CH_3*CHOH.

Table 3.1. *ZPE* and TS_{vib} contributions at 298.15 K to the free energies of adsorbates on the (111) and (100) facets of copper. NH: No coardsorbed hydrogen. HC: High coverage of hydrogen.

Adsorbate	ZPE_{111}	ZPE_{100}	ZPE_{322}	$TS_{vib,111}$	$TS_{vib,100}$	$TS_{vib,322}$
*CH_3CH_2O (NH)	1.837	1.822	1.833	0.304	0.310	0.302
*CH_3CHOH (NH)	1.809	1.794	1.821	0.316	0.277	0.213
*CH_3CH_2O (HC)	2.860	2.487	2.463	0.295	0.394	0.261
*CH_3CHOH (HC)	2.820	2.438	2.432	0.320	0.409	0.371

We have added a solvation correction of -0.38 eV to CH_3*CHOH due to the presence of the OH group, making use of the approximations described elsewhere [107, 120]. Finally, we have used the computational hydrogen (CHE) approach to simulate concerted proton-electron transfers[121]. In this approach, the energetics of H_2(g) rather than that of (H^++e^-) is used as electrochemical reference due to the following relationship in equilibrium: $\mu\left(H^+ + e^-\right) = \frac{1}{2}\mu\left(H_2\right)$.

3.4 Results and discussion

The linear sweep voltammetry (LSV) of the three copper single-crystals shows reduction currents at negative potentials which are mainly due to hydrogen evolution, see Appendix II, Figure AII.2. To probe the reduction of acetaldehyde to ethanol, we need to use online HPLC, since LSV does not show the separated features for acetaldehyde reduction. Figure 3.1 shows the HPLC results for the electrochemical reduction of results in more negative onset potentials, as the coordination number is 7 for the step edge on acetaldehyde on three different copper electrodes and at different pH values. We observe that the onset potential for the formation of ethanol follows the trend Cu(322) > Cu(100) > Cu(111) for both values of pH (see also Figure 3.4). This means that increase in surface coordination the (322) electrode (note that (322) electrodes are also denoted 5(111)×(100), as they have 5-atom wide (111) terraces separated by (100) steps), and the coordination numbers are 8 and 9 on the (100) and (111) terraces, respectively. For instance, at pH 1, the onsets are located at -0.30 ± 0.03 V_{RHE}, -0.54 ± 0.03 V_{RHE} and -0.78 ± 0.03 V_{RHE}, for the three facets.

Note that the equilibrium potential for this reaction is located at 0.24 V_{RHE} at pH 0, and also that it is generally observed that adsorbates bind more strongly to undercoordinated facets [122-125]. These two observations suggest that the adsorbed intermediates of the reduction of acetaldehyde are less stable than acetaldehyde itself under equilibrium conditions. Thus, the applied potential is used to make their adsorption thermodynamically and kinetically favorable. Therefore, the onset of ethanol greatly depends on the stabilization of such intermediates on the electrode surface. In order to gain further insight into the reaction mechanism, we have performed DFT calculations on Cu(111), Cu(100) and Cu(322) in the way described in the Computational Details section. The two possible adsorbed intermediates resulting from the transfer of a proton-electron pair to acetaldehyde are CH_3CH_2O* and CH_3*CHOH. The proposed reduction mechanism in Figure

3.2 includes the reactant and the product, namely acetaldehyde and ethanol, and the most stable adsorbed intermediate, which is CH_3CH_2O*. The adsorption energies in the pathway that goes through the other possible intermediate, CH_3*CHOH, are provided in Figure 3.3. As CH_3CH_2O* is more stable than CH_3CHOH on all facets regardless of the presence or absence of co-adsorbed H*, in the following we focus only on the results for CH_3CH_2O* in Figure 3.2.

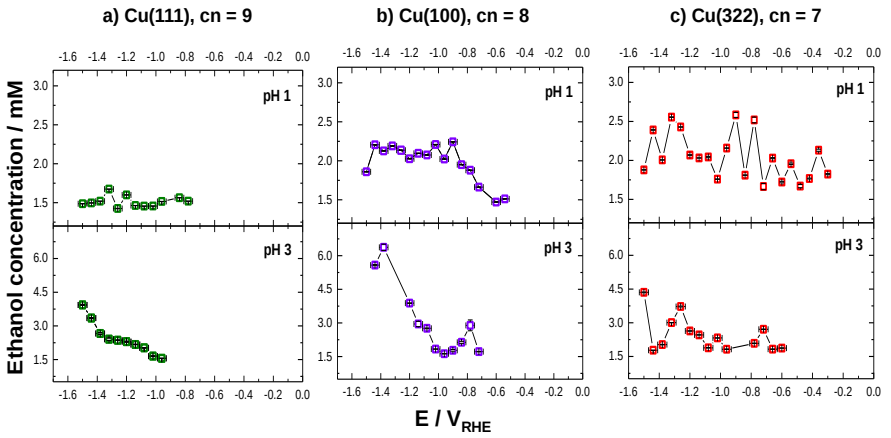

Figure 3.1: Concentration of ethanol produced as a function of potential for the electroreduction of 0.1 M acetaldehyde on three different copper surfaces: a) Cu(111), b) Cu(100), c) Cu(322). The solutions used are: 0.1 M $HClO_4$ (pH 1), and 0.001 M $HClO_4$ + 0. 099 M $KClO_4$ (pH 3). Argon atmosphere. Lines connecting the data points are given as a guide to the eye. An earlier onset of the reaction is associated to surfaces with lower coordination numbers.

The calculations in Figure 3.2.a, which contain only adsorbed CH_3CH_2O* on the slabs, indicate that already at 0 V and in the absence of *H the reduction of acetaldehyde is thermodynamically favorable on the three facets under study. However, this is not what we observe experimentally. In experiments, acetaldehyde reduction takes place in a high-coverage regime of *H, which is included in Figure 3.2.b. Therefore, a high-coverage situation is a more realistic approximation to the experimental environment in which the intermediates of acetaldehyde

reduction ($CH_3CH_2O^*$) compete with those of hydrogen evolution (*H) for active sites at copper surfaces.

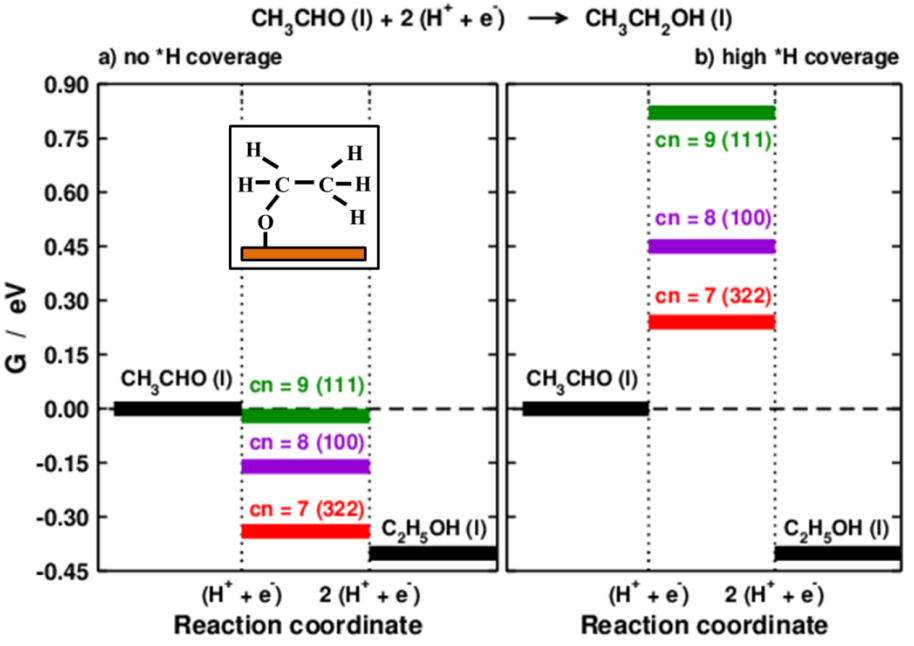

Figure 3.2: Electrochemical reduction of acetaldehyde (CH3CHO) to ethanol (C2H5OH) on various facets of copper at 0 V: Cu(111) (green, cn = 9), Cu(100) (violet, cn = 8) and Cu(322) (red, cn =7). The pathways proceed via CH3CH2O* (see the inset). a) With no *H coverage. b) With high *H coverage.

The observed effect of hydrogen coadsorption on all facets is a weakening of the metal-adsorbate interactions, which ultimately results in predicted onset potentials which are far from the equilibrium potential: -0.28 V for Cu(322), -0.45 V for Cu(100) and -0.82 V for Cu(111), in very reasonable agreement with experiment. Note in passing that Peterson and co-workers have studied the opposite effect, namely the effect of *CO coverage on hydrogen evolution and found that it systematically weakens the adsorption energies of *H on various metals [126]. Therefore, the coadsorption of *H and *CO weakens the adsorption energies of both species.

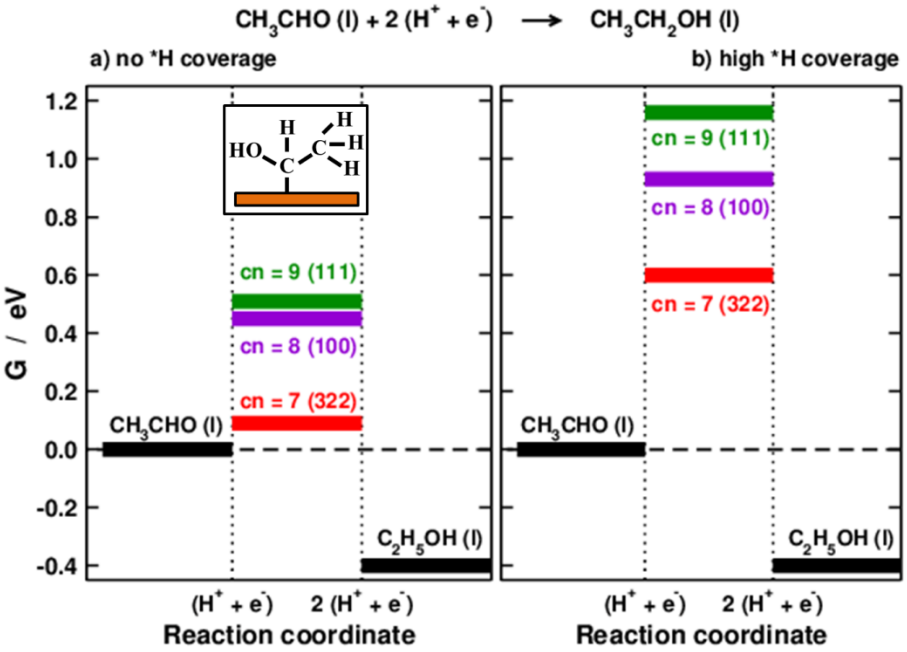

Figure 3.3: Electrochemical reduction of acetaldehyde (CH_3CHO) to ethanol (C_2H_5OH) on various facets of copper at 0 V: Cu(111) (green, cn = 9), Cu(100) (violet, cn = 8) and Cu(322) (red, cn =7). The pathways proceed via CH_3*CHOH (see the inset). a) With no *H coverage. b) With high *H coverage.

According to Figure 3.2.b and in line with the experimental observations in Figure 3.1, the adsorption energies of CH_3CH_2O* at 0 V are higher than the energetic levels of acetaldehyde and ethanol on all facets. This means that the first proton-electron transfer is uphill in energy, while the second one is downhill. Thus, the predicted onset potentials on all facets in Figure 3.2.b correspond to the energy difference between acetaldehyde and the adsorbed intermediates.

As observed in the experiments in Figure 3.1, copper facets with lower coordination numbers exhibit less negative onset potentials, which can be intuitively understood as follows: in general, it is observed that adsorbates are more strongly bound to undercoordinated sites [122-125],

which implies that the step edge on the (322) facet, where the coordination number is 7, will display more negative adsorption energies for CH_3CH_2O* compared to the (100) and (111) facets, where the coordination numbers are 8 and 9, respectively. Since these endothermic adsorption energies are more positive than the level of acetaldehyde (see Figure 3.2), stronger adsorption energies imply earlier onset potentials. In summary, our high-coverage DFT calculations confirm the structure-sensitive reduction of acetaldehyde to ethanol observed experimentally, and show that the mechanism proceeds on the three facets via CH_3CH_2O*, which becomes more stable as the coordination of the adsorption sites is decreased. The calculations also show the importance of considering the co-adsorption of H* in reaching good agreement with experiments. We have summarized the experimental and theoretical trends in Figures 3.1, 3.2 and 3.3 in Figure 3.4. This figure contains the adsorption energies of CH_3CH_2O* and CH_3*CHOH with and without coadsorbed *H and the additive inverse of the experimental onset potentials which, according to the results in Figure 3.1, corresponds to experimental free energy of adsorption of the adsorbed intermediate of acetaldehyde reduction.

3.5 Mechanistic implications

It is important to discuss the mechanistic implications of our observations for the reduction of CO/CO_2 to ethanol and other C_2 products such as ethylene. We have previously proposed the mechanism shown in Figure 3.5 for the reduction of CO to C_2 species on Cu(100) on the basis of DFT calculations [107]. In that mechanism, ethanol, acetaldehyde and ethylene share the same intermediates up to the fifth proton-electron transfer, which is supported by the experiments of Hori and coworkers, who observed that the nature of the metallic cations from the electrolyte affects similarly the Faradaic efficiencies of ethylene and ethanol production [65].

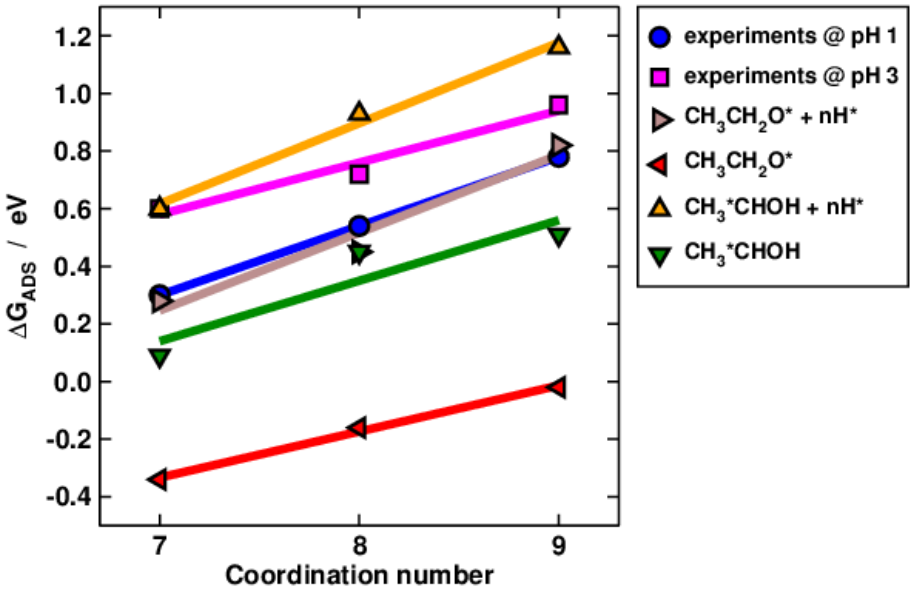

Figure 3.4: Experimental (●, ■) and theoretical (►, ◄, ▲, ▼) trends in adsorption energies of the adsorbed intermediates of acetaldehyde reduction as a function of the coordination number of the active sites on Cu(322) (step edge, cn = 7), Cu(100) (cn = 8), and Cu(111) (cn = 9).

The product of the fifth proton-electron transfer is the "selectivity-determining" intermediate (SDI in Figure 3.5). The sixth proton-electron transfer favors the formation of ethylene (orange pathway in Figure 3.5) over acetaldehyde (grey pathway in Figure 3.5) at the onset of ethylene formation, that is at -0.4 V_{RHE} [107]. The results in Figures 3.1 and 3.2 indicate that the onset of acetaldehyde reduction to ethanol requires -0.54 V_{RHE} on Cu(100) (-0.45 V from DFT calculations). Such onset for the formation of ethanol from acetaldehyde is in contrast to previous experimental and theoretical results on the reduction of ethylene oxide to ethylene on polycrystalline copper, the onset of which is less negative than -0.4 V_{RHE} (-0.35 V from the backward scan in experiments and -0.33 V from DFT calculations on Cu(100)) [107, 109]. Unlike acetaldehyde reduction, the potential-determining step for ethylene oxide reduction is the second proton-electron transfer, which implies that desorption of adsorbed intermediates limits the onset of the reaction. In the case of a

desorption-limited reaction, structure sensitivity affects the trends in onset potentials differently: undercoordinated sites binding adsorbates more strongly increase the onset potential.

The conjunction of the findings for ethylene oxide and acetaldehyde reduction suggests that, although ethylene and ethanol share common intermediates in the early stages of CO/CO_2 reduction, the protonation of the SDI favours ethylene formation compared to ethanol formation on Cu(100). Importantly, we have shown here that undercoordinated sites at stepped surfaces are able to lower those barriers by virtue of their stronger adsorption energies. Step sites, on the other hand, affect adversely the production of ethylene on Cu(100).

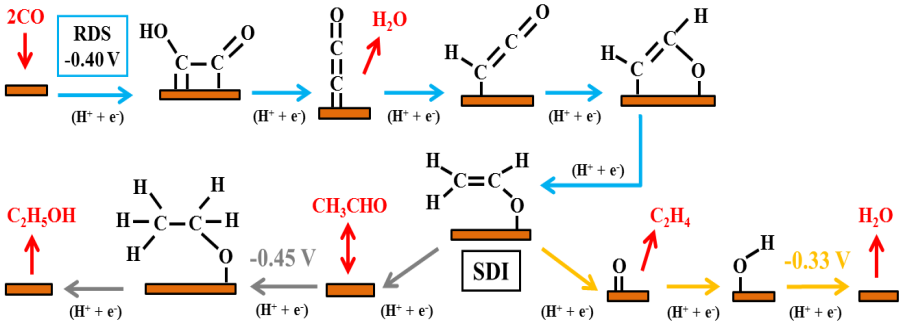

Figure 3.5: Mechanism of the electrochemical reduction of CO on copper to C_2 species on Cu(100), adapted from ref. [107]. The pathways for the production of acetaldehyde, ethanol and ethylene are identical up to the fifth proton-electron transfer (blue arrows). The rate-determining step (RDS at -0.40 V) is the first proton-electron transfer and CH_2CHO^* is the selectivity-determining intermediate (SDI). Protonation of the SDI on the β-C requires -0.45 V and leads to acetaldehyde and ethanol (grey arrows). Protonation on the α-C requires -0.33 V and leads to ethylene and water (orange arrows). On Cu(100) the protonation of the SDI is inclined towards the ethylene pathway (orange arrows).

3.6 Conclusions

Elucidation of the reaction mechanism of CO/CO_2 reduction to C_2 species is not trivial, as it involves the transfer of several proton-electron pairs and numerous adsorbed intermediates. A possible way of simplifying the problem is to analyze separate reactions involving fewer proton-electron transfers. In that vein, we have considered here the structure-sensitive reduction of acetaldehyde to ethanol on copper, which corresponds to the late stages of CO/CO_2 reduction to ethanol. Our results suggest that ethanol formation is more favourable on open copper surfaces, which is explained by the preference of $CH_3CH_2O^*$ for undercoordinated sites. Therefore, a plausible way of inclining the selectivity of copper electrodes towards the formation of ethanol from CO/CO_2 is the use of undercoordinated square sites: square ensembles because they catalyze the formation of C-C bonds, and undercoordinated sites because they incline the selectivity towards ethanol instead of ethylene.